Journal of Computational and Applied Mechanics, Vol. 3., No. 1., (2002), pp. 61–84

EXAMINATION OF CONTACT OPTIMIZATION AND WEARING PROBLEMS

István Páczelt and Attila Baksa
Department of Mechanics, University of Miskolc
3515 Miskolc-Egyetemváros, Hungary
mechpacz@uni-miskolc.hu and mechab@uni-miskolc.hu

[Received: April 22, 2002]

Dedicated to Professor Gyula Béda on the occasion of his seventieth birthday

Abstract. A system of elastic bodies is examined. It is assumed that the displacements and deformations are small. Firstly, the minimum of maximum pressure and other mechanical values (torque, frictional power loss) are sought by controlling the distribution of contact pressure. Secondly, the optimization problem for roller bearings in rolling state will be discussed and the optimization problem for the wearing process will be formulated as well. For the solution of the optimization problems special iterational algorithms have been developed. In order to solve the contact problem we use both the total potential energy with augmented Lagrangian technique and the modified complementary energy. The p-version of the finite element method is applied for the first problem type, while in the second case an iterational algorithm is developed which includes Kalker's *KOMBI* program. Numerical examples demonstrate the efficiency of the proposed iterational procedure.

Mathematical Subject Classification: 74M15, 74P99, 74S05
Keywords: contact problems, optimization, p-version FEM, wearing process

1. Introduction

The stress state of machine parts is strongly influenced by their geometrical shapes and forms. The optimum design of elements of different bearings, machine tool guides, bars, etc., needs special considerations to avoid singularities and to improve the strength endurance. In optimization problems the design parameters are usually concerned with material parameters, shape, characteristic dimensions, supports, loads, inner links, reinforcement and topology (see Mróz [1]). In engineering practice, connections between machine elements are frequently modelled as unilateral contact problems. Comparatively few studies can be found in the literature for contact optimization [2], [3]. The thorough mathematical investigation of the subject can be found in [4]. The controlling technique of contact pressure distribution is employed for the shape optimization problem of cylindrical bodies using h- and p-version of the finite element method without friction in [5], [6] and with friction in [7]. Work [8] gives a contribution to the solution for practical problems by controlling the contact

pressure distribution when one of the bodies has rigid body translation and rotation. The question of round off is examined in [9] for roller bearings without friction.

Contact pressure optimization is studied for the problem of an elastic punch and a rigid target within the framework of linear elasticity in [10]-[13]. In many earlier works [14]-[16] the maximum contact pressure was chosen to be the objective function, but it was not differentiable. Articles [10], [11], [13] and [17] use the total potential energy as a cost function and the integral of the gap function as the ISO-parametric constraint.

Approximately constant contact pressure distribution has been achieved in [15], [16] by appropriate shape optimization for axially symmetric bodies, assuming that the change in radius has no effect on the stiffness and compliance matrices.

Discretization of the domain with p-version finite elements is advantageous [18], since it results in fast convergence, and high order mapping assures accurate geometry for shape optimization.

Five types of mechanical contact problems will be examined:

1. Minimization of the maximum of contact pressure.
2. Maximization of rigid body displacement.
3. Maximization of torque or the contact resultant force between the bodies.
4. Minimization of frictional power loss (wearing values) between machine elements.
5. Optimization of roller shape by controlling the contact pressure distribution.

In case 5 the effect of frictional stress, which arises during the rolling motion, is taken into account. In cases 2, 3 and 5 the Mises equivalent stress is kept under a prescribed limit in addition to the control of contact pressure.

In the optimization of roller shape, the influence matrix is derived from the solution of the elastic half-space problem [19], and the mirror technique is also applied in this program [9].

The p-version of the finite element method is used in the first four types of the optimization problems.

2. Contact conditions

The contact of two elastic bodies ($\alpha = 1, 2$) is examined here. It is assumed that the displacements and deformation are small. The body volumes V^α are bounded by surfaces S^α, which can be separated into S_p^α, S_u^α – on which the surface traction is $\widetilde{\mathbf{p}}$ and the displacement $\mathbf{u}_0$ is given – and into S_c^α on which there could be unilateral contact (see Figure 1). The Signorini type contact conditions are assumed in normal direction $\mathbf{n}_c$, where $\mathbf{n}_c = -\mathbf{n}^2 \cong \mathbf{n}^1$.

The normal stress on the surface S_c^α is $\sigma_N^\alpha = \mathbf{n}^\alpha \cdot \boldsymbol{\sigma}^\alpha \cdot \mathbf{n}^\alpha$, where $\boldsymbol{\sigma}^\alpha$ is the stress tensor. After deformation the gap in the direction $\mathbf{n}_c$ is

$$d = u_N^2 - u_N^1 + h \tag{2.1}$$

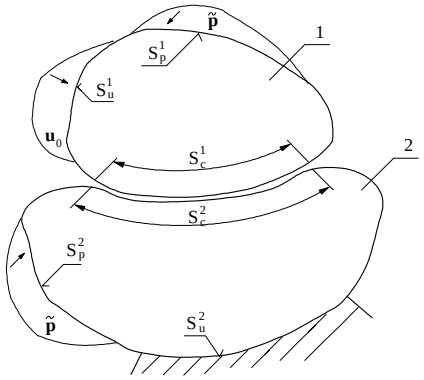

Figure 1. The contact between two bodies

where $u_N^\alpha = \mathbf{u}^\alpha \cdot \mathbf{n}_c$ and h is the initial gap – see Figure 2 for further details.

Let

$$p = -\sigma_N^1 = -\sigma_N^2 \tag{2.2}$$

be the contact pressure. It is clear that there is contact if the following conditions are fulfilled

$$d = 0\,, \qquad p \geq 0 \qquad \mathbf{x} \in \Omega_p\,, \tag{2.3a}$$

and there is separation if

$$d \geq 0\,, \qquad p = 0 \qquad \mathbf{x} \in \Omega_0\,, \tag{2.3b}$$

that is

$$p \cdot d = 0\,, \qquad \mathbf{x} \in S_c = \Omega = \Omega_p \cup \Omega_0\,. \tag{2.3c}$$

To calculate the effects of friction, the slip between the contacting bodies is also to

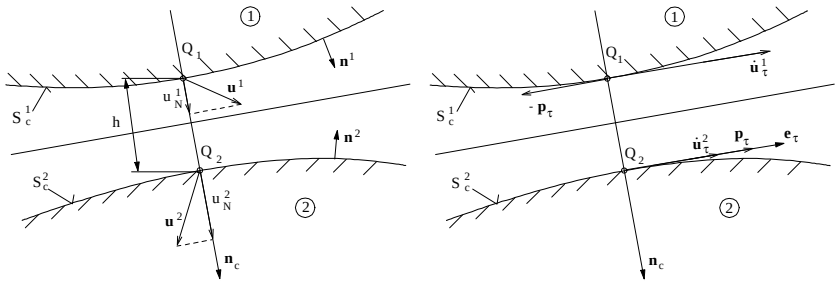

Figure 2. Contact and separation

be defined. The Coulomb dry friction model is employed henceforth. The relative slip in tangential direction is formulated as

$$\dot{\mathbf{u}}_\tau = \dot{\mathbf{u}}_\tau^1 - \dot{\mathbf{u}}_\tau^2\,, \tag{2.4}$$

where $\dot{\mathbf{u}}_\tau^\alpha$ is the tangential velocity in the body α. The adhesion zone of the contact region is characterized by the following conditions

$$\|\mathbf{p}_\tau\| \le \mu\, p\,, \qquad \dot{\mathbf{u}}_\tau = \mathbf{0}\,, \tag{2.5a}$$

where

$$\mathbf{p}_\tau = -\sigma^1 \cdot \mathbf{n}^1 - p\,\mathbf{n}_c = \sigma^2 \cdot \mathbf{n}_c - p\,\mathbf{n}_c \equiv \mathbf{p} - p\,\mathbf{n}_c\,. \tag{2.5b}$$

In the slip domain the traction in tangential direction is given as

$$\mathbf{p}_\tau = \mu\, p \frac{\dot{\mathbf{u}}_\tau}{\|\dot{\mathbf{u}}_\tau\|}\,, \tag{2.5c}$$

where $\mathbf{p}_\tau$ is calculated for the lower body, namely the second body in our case.

The boundary value problem is solved by making use of variational principles [20] by which we mean the modified complementary energy and potential energy with augmented Lagrangian technique [8], [24].

3. Optimization problems

3.1. **Control of the contact pressure.** The expected aim is achieved by changing the shape of the proposed zone of contact domain in the types of contact optimization tasks considered. Some works can be found in the references where the shape of the contacting bodies is changed on the surfaces which are out of the contact zone, such as [21], [22] and [23].

In our optimization problems it is assumed that the bodies are in contact in the whole sub-domain Ω_c of the contact zone $S_c = \Omega$, where Ω_c is called the control sub-domain. The contact surface is modified so that the following function holds true for the contact pressure

$$p(\mathbf{x}) = v(\mathbf{x})\, p_{\max}\,, \qquad \mathbf{x} \in \Omega_c\,, \tag{3.1}$$

where the control function we have chosen must satisfy the condition $0 \le v(\mathbf{x}) \le 1$, and

$$p_{\max} = \max\, p(\mathbf{x})\,, \qquad \mathbf{x} = [s,t]\,, \tag{3.2}$$

where s and t are surface co-ordinates in the region Ω. In the sub-domain Ω_{nc} ($\Omega =$

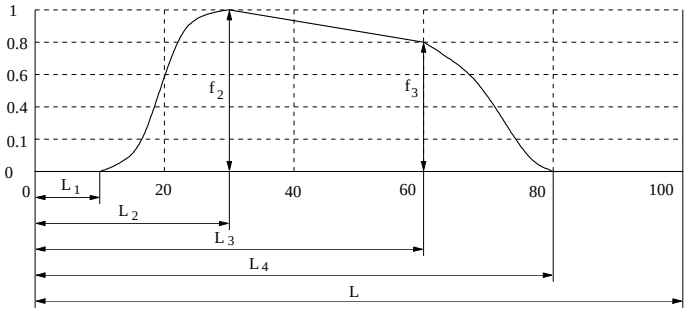

Figure 3. $V(s)$ function

$\Omega_c \cup \Omega_{nc}$), where the pressure is not controlled, the fulfillment of the following inequality is required

$$\chi(\mathbf{x}) = v(\mathbf{x})p_{\max} - p(\mathbf{x}) \geq 0, \qquad \mathbf{x} \in \Omega_{nc}. \tag{3.3}$$

Let us define a function $V(s)$ of class C^1 in the sub-region Ω_c (see Figure 3)

$$V^* = V^*(s) = f_2 + (f_3 - f_2)\frac{s - L_2}{L_3 - L_2} \tag{3.4}$$

$$V(s) = 0\,, \qquad 0 \leq s \leq L_1$$

$$V(s) = V^* \left\{ 3 \left[\frac{s - L_1}{L_2 - L_1} \right]^2 - 2 \left[\frac{s - L_1}{L_2 - L_1} \right]^3 \right\}, \qquad L_1 \leq s \leq L_2$$

$$V(s) = V^*, \qquad L_2 \leq s \leq L_3$$

$$V(s) = V^* \left\{ 1 - 3 \left[\frac{s - L_3}{L_4 - L_3} \right]^2 + 2 \left[\frac{s - L_3}{L_4 - L_3} \right]^3 \right\}, \qquad L_3 \leq s \leq L_4$$

$$V(s) = 0\,, \qquad L_4 \leq s \leq L,$$

where parameters $f_2, f_3, L_j, j = 1, \ldots, 4$ are fixed or some of these are calculated in the optimization process. In this case $\frac{dV}{ds} = 0$ at $s = L_1, s = L_4$, and also if $f_2 = f_3 = 1$ at points $s = L_2, s = L_3$.

For two dimensional contact problems $v(s) = V(s)$ in Ω. For three- dimensional problems it is assumed that the upper body has a translation and a rigid body rotation, Ω_c is a line s, and the rotation vector is perpendicular to this line. The control function along the curve s has the following form

$$v(s) = V(s) \left[1 + B \left(\frac{s}{L} \right)^n \right], \tag{3.5}$$

and along direction t $\widetilde{v}(t) = 1$, that is

$$v(\mathbf{x}) = v(s)\widetilde{v}(t). \tag{3.6}$$

Value B is calculated from equilibrium equations for the first body, where $10 \leq n \leq 15$ [8].

3.2. **Contact optimization for axisymmetric bodies.**

3.2.1. *Solving the contact problems with iteration.* Firstly, the arising equivalent stress is not taken into account in most of the tasks investigated. The optimal shape is determined besides the prescribed parameters (L_i, $i = 1, \ldots, 4$).

The solution of the problem is found with the iterational method, introduced in [8]. This method is labelled as 1^{st} *type iteration.*

Secondly, the Mises equivalent stress σ_{eq} must be under a prescribed ultimate stress σ_U

$$\sigma_{eq} \leq \sigma_U. \tag{3.7}$$

When the optimization problem includes (3.7) as an additional condition, the solution requires another iteration, labelled as 2^{nd} *type iteration.* These problems are classified

into two main groups. The first one is when a kinetic or dynamic quantity is maximized (for example the displacement of the upper punch or the contact force between the bodies). The second one is when one of the control parameters (see Figure 3) is minimized or maximized.

The 2^{nd} *type iteration* is built up in the following way. The quantity searched for is f. During the iteration the value of f is changed. The iteration variable is istep, and the value of f is calculated by

$$f = f_0 \cdot \mathsf{istep}\,, \tag{3.8}$$

where f_0 is chosen in advance. The optimization problem is solved by the 1^{st} *type iteration* with the fixed f. In each istep a new shape is determined for the upper body.

The Mises equivalent stress σ_{eq} is calculated in the Gaussian integral points of the finite elements and in the border points as well: $(\xi = -1, \xi_1, \ldots, \xi_{NG}, 1)$, $(\eta = -1, \eta_1, \ldots, \eta_{NG}, 1)$, where ξ, η are the local normal co-ordinates, and NG is the number of integration points along the direction ξ or η. When $\sigma_{eq} > \sigma_U$ in any control points, then $f = f^{**}$ and in the previous step $f = f^*$. The optimal f^{opt} is searched for in the interval $f^* < f^{opt} < f^{**}$ by the following linearization process:

$$f^{opt^{(i)}} = f^* + (f^{**^{(i)}} - f^*) \cdot \frac{\sigma_U - \sigma^*_{eq}}{\sigma^{**^{(i)}}_{eq} - \sigma^*_{eq}} \qquad i = 1, 2, \ldots \tag{3.9}$$

where $f^{**^{(1)}} = f^{**}$, $\sigma^{**^{(1)}}_{eq} = \sigma^{**}_{eq}$, σ^*_{eq} is the maximum value of the Mises equivalent stress calculated by f^* similarly to the value of σ^{**}_{eq}. The iterational process will run until

$$\frac{\left|\sigma_U - \sigma^{**^{(i)}}_{eq}\right|}{\sigma_U} \leq 0.015. \tag{3.10}$$

3.2.2. *Optimization problems examined.* In the present examination axisymmetric bodies (see Figure 4) are discretized by p-extension elements [18].

The following problems have been analyzed:

P1: The vertical displacement w_0 is prescribed on the top surface of the punch. Using the control function with given parameters L_j, $(j = 1, \ldots, 4)$, the shape optimization is performed on the punch keeping its unloaded original length that is fixed in axial direction. Introducing a new variable $s = R - R_b$, and Δh for the gap function, the optimization problem [8] is formulated as

$$\begin{aligned} \min \Big\{ p_{\max} \,\Big|\, & p \geq 0,\ d = d(p, \Delta h) = 0\,, \\ & \chi = v(s)\, p_{\max} - p(s) = 0,\ \min \Delta h = 0 \Big\}. \end{aligned} \tag{3.11}$$

The problem is solved by the 1^{st} *type iteration.*

P2: This is the problem where the additional constraint (3.7) is to be satisfied during the optimization process. So the value of displacement w_0 on the top surface

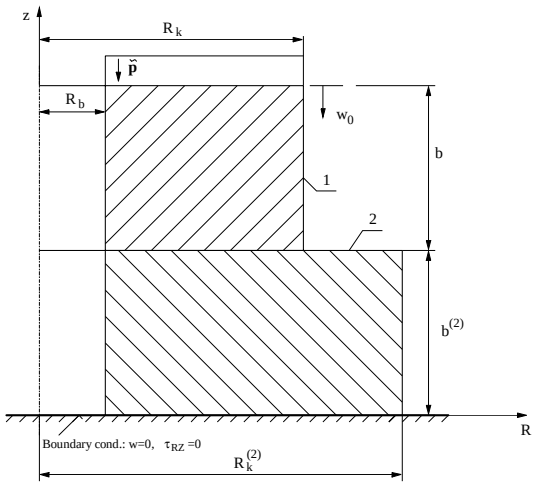

Figure 4. Punch problem of axially symmetric bodies

of the upper body must be maximized, thus the problem to be solved can be described as follows

$$\max\Big\{w_0\,\Big|\,\min\big\{p_{\max}\,\big|\,p\geq 0,\, d=d(p,\Delta h)=0\,,\\ \chi=0,\,\min\Delta h=0\big\},\sigma_{eq}\leq\sigma_U\Big\}. \tag{3.12}$$

in which the inner optimization problem is calculated by the 1^{st} *type iteration*, while the 2^{nd} *type iteration* is used for solving the outer task. In equation (3.9) the quantity searched for is $f = w_0$.

P3: Applying the given displacement w_0 and the control function of problem P1, shape optimization is performed on the punch resulting in a given value of compressing force F_p [8].

$$\min\Big\{p_{\max}\,\Big|\,p\geq 0,\, d=d(p,\Delta h)=0,\,\chi=0,\,F_p=2\pi\int\limits_{R_b}^{R_k}R\,p\,dR\Big\}. \tag{3.13}$$

P4: When the constraint of the Mises equivalent stress is kept, the value of F_p cannot be chosen at will, its maximum value will be presented as an additional unknown variable. The problem to be solved is therefore the following

$$\max\Big\{F_p\,\Big|\,\min\big\{p_{\max}\,\big|\,p\geq 0,\, d=d(p,\Delta h)=0,\,\chi=0\big\},\,\sigma_{eq}\leq\sigma_U\Big\}. \tag{3.14}$$

Figure 5 shows an example for this problem, with the following material properties: Young modulus: $E = 2\cdot 10^5\,MPa$, Poisson ratio: $\nu = 0.3$ and geometrical data $R_b = 20\,mm$, $R_k = 120\,mm$, $R_k^{(2)} = 140\,mm$, $b = b^{(2)} = 50\,mm$. The parameters of the control function in (3.4) are $L_1 = 0\,mm$, $L_2 = 4\,mm$, $L_3 =$

$96\,mm$, $L_4 = 100\,mm$. The prescribed displacement on the top surface of the upper body is $w_0 = 0.1\,mm$. Let the value of f_0 in equation (3.8) be

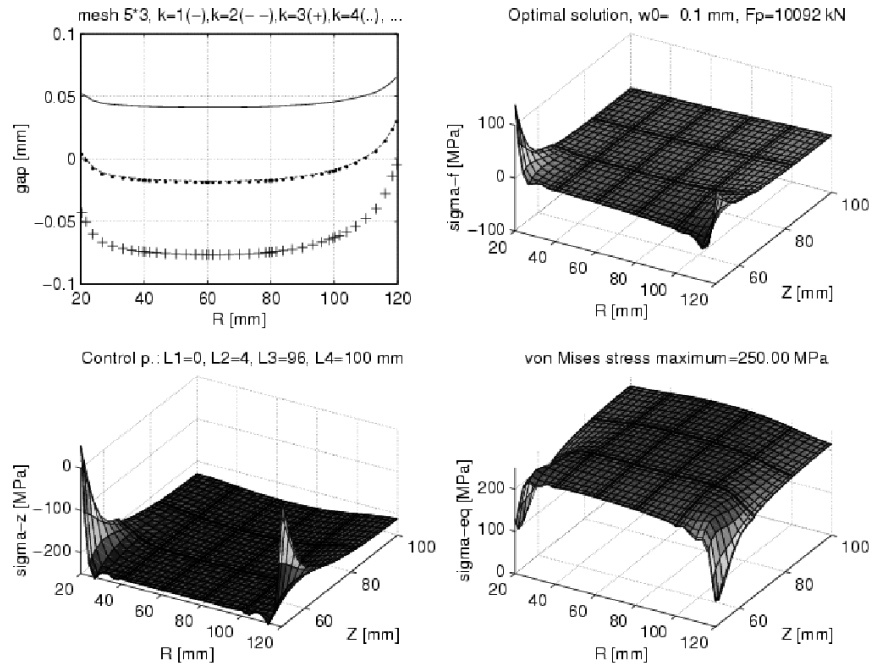

Figure 5. Gap and stress distribution for Problem P4

$f_0 = F_0 = 5000\,kN$ fir which the contact force is $F_p = F_0 \cdot \mathsf{istep}$ in the 2^{nd} *type iteration*. In Figure 5 the upper left picture illustrates the gap during the iterations ($k = \mathsf{istep}$). $\sigma_{eq} < \sigma_U$ in the first two iterations ($k = 1, 2$), but for $k > 2$ then σ_{eq} is significantly more than σ_U. In this example the number of iterations in (3.9) is two. The result shows that the height of the upper part must be extended, i.e., the initial gap between the bodies is a negative value in the interval $20 \le R \le 110$. The maximum of the compressing force F_p is also calculated and is equal to $= 10092\,kN$.

P5: The punch is loaded by a constant pressure $\widetilde{p}$ on its top surface. The resultant is $F_0 = \pi(R_k^2 - R_b^2)\widetilde{p}$. The torque M_T should be maximized

$$\frac{M_T}{\mu} = \int_{R_b}^{R_k} 2\pi R^2\, dR\,, \tag{3.15}$$

where μ is the coefficient of friction. It is evident that the maximum torque is achieved when only the outer corner of the punch ($R = R_k$) is in contact, and the minimum value is observed if any of the inner corners of the punch ($R = R_b$) is in contact. In order to have a smooth stress distribution the shape of

the punch is determined using a control function given in terms of the parameters $(L_2 - L_1), L_3$ where the latter has a fixed value and L_4 is also fixed. The control of the discretization of contact pressure is calculated from the following equation:

$$\begin{aligned}\chi = \chi(s, p, L_1) =& v(s, L_1, L_2(L_1), L_3 \text{ and } L_4 \text{ are fixed})\, p_{\max} \\ & - p(s, L_1) = v(s, L_1)\, p_{\max} - p(s, L_1) = 0\,,\end{aligned} \tag{3.16}$$

that is

$$p(s, L_1) = v(s, L_1)\, p_{\max}\,. \tag{3.17}$$

The equilibrium equation for the upper body is

$$F = F(L_1, p_{\max} \text{ is fixed}) = F_0 - 2\pi \int_{R_b}^{R_k} R\, v(R - R_b, L_1)\, p_{\max}\, dR = 0\,. \tag{3.18}$$

The value of L_1 can be determined from equation (3.18) because the maximum value of the contact pressure $p_{\max}$ is prescribed.

The optimization problem is formulated as follows

$$\begin{aligned}\max \Big\{ \frac{M_T}{\mu} \,\Big|\, & p = p(s, L_1) \geq 0,\ d = d(p, \Delta h) = 0\,, \\ & \chi = \chi(s, p, L_1) = 0,\ F = F(L_1, p_{\max} \text{ is fixed}),\ \min \Delta h = 0 \Big\},\end{aligned} \tag{3.19}$$

where parameters L_1, Δh, p are unknown [8].

P6: When the additional stress condition (3.7) is kept, the value of $p_{\max}$ cannot be fixed in advance. The solution should be searched for by maximizing length L_1, and the problem to be solved is formulated as follows

$$\begin{aligned}\max_{L_1} \Big\{ \frac{M_T}{\mu} \,\Big|\, & p = p(s, p_{\max}(L_1)) \geq 0,\ d = d(p, \Delta h) = 0, \chi = \chi(s, p, L_1) = 0\,, \\ & F = F(p_{\max}(L_1)) = 0,\ \min \Delta h = 0,\ , \sigma_{eq} \leq \sigma_U \Big\}.\end{aligned} \tag{3.20}$$

During the optimization process the distance L_1 is changed by $\Delta L_1 = \frac{L_3 - L_1}{10} = \frac{96-4}{10}$, where L_3, L_4 are the control parameters in the initial state, i.e. (istep $= 1$). The optimal length is L_1^{opt}, which is computed in the $L_1^* < L_1^{opt} < L_1^{**}$ interval using the iteration with linear approximation according to (3.9).

Figure 6 shows the results of a numerical example and Figure 7 shows the shape of the punch during the iteration. The load of the upper body is $\widetilde{p} = 100\, MPa$. After the solution of the optimization problem the results are the following, $L_1^{\text{opt}} = 19.42\, mm$, $L_2 = L_1^{\text{opt}} + 4$, $\frac{M_T}{\mu} = 377.68 \cdot 10^6\, Nmm$. Figure 6 shows the solution for the original construction, i.e., when there is no initial gap between the contacting bodies. The number of iterations istep varies from 0 to 6. If (istep $= 1$), the control parameters are $L_1 = 0\, mm$, $L_2 = 4\, mm$, $L_3 = 96\, mm$, $L_4 = 100\, mm$.

Since the elements around the point with co-ordinates $R = R_k$, $z = b^{(2)}$ in the lower body are not small, the solution cannot give as a high value for σ_{eq} in istep $= 0$ as is expected. Theoretically this point shows singularity with respect

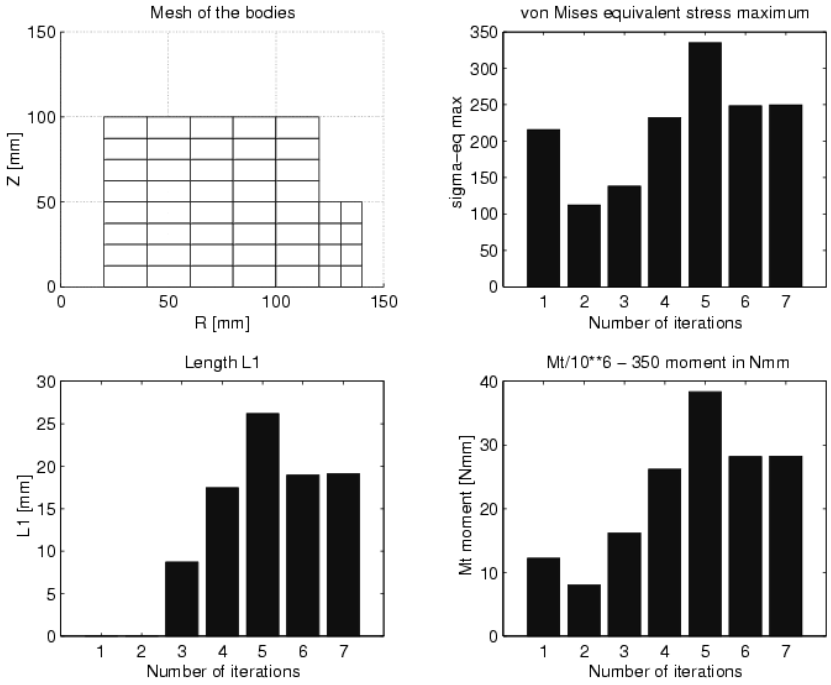

Figure 6. Results of optimization problem P6 (Number of iterations $=$ istep $+\,1$)

to the stress state. In our investigation the control of the contact pressure gives the stress state without any singularity, so large elements are applicable.

Choosing different loads $\widetilde{p}$ the results are shown in Table 1. It is observed that the pressure $\widetilde{p}$ is changing linearly however the torque is not increased in that way. The 2^{nd} *type iteration* is controlled by keeping the inequality (3.10).

$\widetilde{\mathbf{p}}\ [MPa]$	$\mathbf{L_1}\ [mm]$	$\frac{\mathbf{M_T}}{\mu} \cdot 10^{-6}\ [Nmm]$	$\mathbf{p}_{\max}\ [MPa]$	$\max \sigma_{\mathbf{eq}}\ [MPa]$
40	48.932	169.646	62.968	249.98
60	33.454	238.869	77.468	252.69
80	24.569	307.771	95.210	248.12
100	19.418	377.677	114.480	249.35

Table 1. Results for problem P6 with different loads

P7: The relative angular velocity ω of the punch is given. The shape of the contact surface is optimized in order to minimize the frictional power loss by applying the control function with parameters $L_1 = 0\,mm$, L_2 is a fixed value and $L_4 - L_3$ are

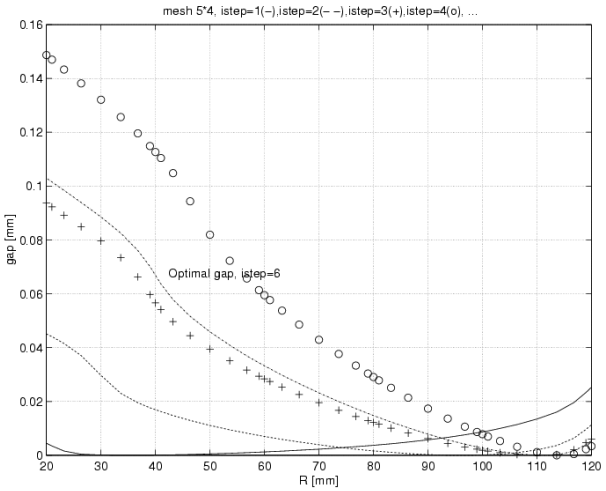

Figure 7. Gaps during the optimization problem P6

given values. The power loss is written as

$$D = \int_{R_b}^{R_k} 2\pi R\,\omega\,\mu\,R\,dR = M_T\,\omega\,. \tag{3.21}$$

The closer the location of the resultant of the contact pressure to radius R_b the smaller the frictional power loss, so the optimization problem [8] is expressed as

$$\min\Big\{\frac{D}{\mu\,\omega}\,\Big|\,p = p(s,L_4) \geq 0,\; d = d(p,\Delta h) = 0,\; F = F(L_4, p_{\max}\,\mathsf{is\ fixed}) = 0\,,$$
$$\chi = v(s,L_1,L_2\,\mathsf{is\ fixed}, L_3(L_4), L_4)\,p_{\max} - p(s,L_4) = 0,\; \min\Delta h = 0\Big\}\,, \tag{3.22}$$

where parameters L_4, Δh and p are unknown if $p_{\max}$ is given.

P8: In this case the additional condition (3.7) is valid, and the length L_4 is minimized during the process of optimization.

$$\min_{L_4}\Big\{\frac{D}{\mu\,\omega}\,\Big|\,p = p(s,p_{\max}(L_4)) \geq 0,\; d = d(p,\Delta h) = 0,\; \chi = \chi(s,p,L_4) = 0\,,$$
$$F = F(p_{\max}(L_4)) = 0,\; \min\Delta h = 0,\; ,\sigma_{eq} \geq \sigma_U\Big\}. \tag{3.23}$$

The train of thought in this iteration is the same as for problem P6. The results are shown in Figure 8. Stress distribution is illustrated in Figure 9. The applied load is $\widetilde{p} = 100\,MPa$ and the results are the following: optimized length is $L_4 = 93,90\,mm$, $L_1 = L_2 = 0\,mm$, $L_3 = L_4 - 4$ and $\frac{D}{\mu\omega} = 337.09 \cdot 10^6\,Nmm$.

During the calculations the initially uniform finite element mesh is modified automatically by the program. To ensure the oscillation-proof results for stress

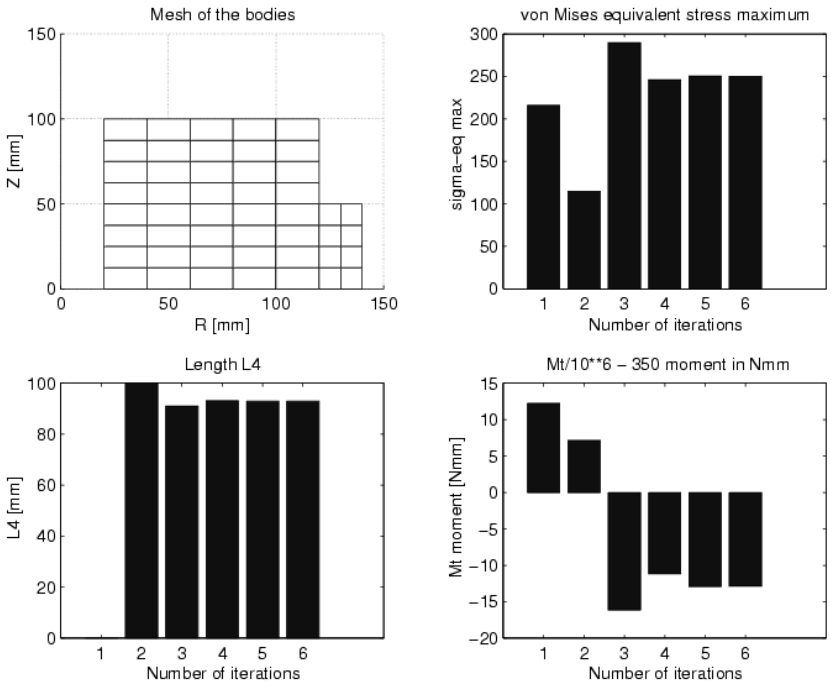

Figure 8. Results of optimization problem P8

distribution intervals $L_3 \leq s \leq L_4$ and $L_4 \leq s \leq L$ are divided into small elements. The contact zone is monitored from the right border point of the second finite element starting at the outer radius of the upper body.

$\widetilde{\mathbf{p}}\ [MPa]$	$\mathbf{L_4}\ [mm]$	$\frac{\mathbf{D}}{\mu\omega} \cdot 10^{-6}\ [Nmm]$	$\mathbf{p}_{\max}\ [MPa]$	$\max \sigma_{\mathbf{eq}}\ [MPa]$
40	78.15	116.839	63.29	249.18
60	86.81	190.064	79.34	247.47
80	91.27	263.595	97.06	247.64
100	93.90	337.091	115.45	250.46

Table 2. Results for problem P8 with different loads

For different loads $\widetilde{p}$ the results are shown in Table 2. The initial control parameters for optimization are $L_1 = L_2 = 0\,mm$, $L_3 = 96\,mm$, $L_4 = 100\,mm$.

P9: In the wearing process the wearing velocity has the following form

$$\dot{w} = c(\mu p)^a ||\dot{\mathbf{u}}_\tau||^b, \qquad \mathbf{x} \in S_c\,, \tag{3.24}$$

where a, b, c are parameters resulting from experiment [25] and $\dot{\mathbf{u}}_\tau$ stores the relative velocity in the tangential direction. The rate of wear is calculated by

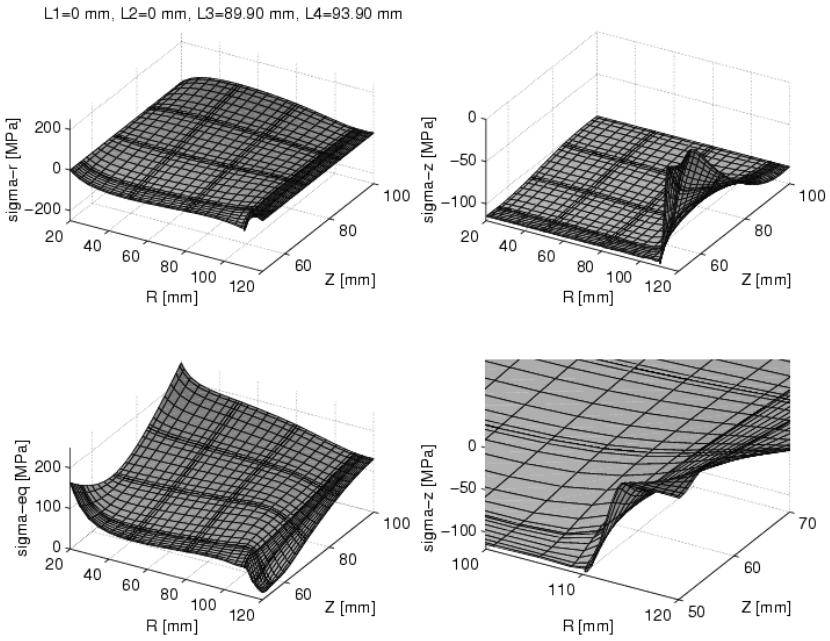

Figure 9. Stress distribution of optimization problem P8

the following formula

$$\dot{W} = \int_{S_c} \dot{w}\, dS\,. \tag{3.25}$$

If $||\dot{\mathbf{u}}_\tau|| = R\omega$ and $a = b = 1$, then

$$\dot{W} = \frac{D}{c} \tag{3.26}$$

that is, the minimization problem for $\dot{W}$ is equivalent to formula (3.23). In another case a strongly nonlinear optimization problem is obtained because the objective function is nonlinear as well.

3.3. **Optimal shape design of rollers.** Rolling elements can be found in a number of engineering equipment. Their long overall lifetime requires keeping stresses at a low and smooth value.

A number of papers [9], [25]-[28] are devoted to the issue of roller rounding-off. In these papers, except for the last one, the radius of rounding-off is given, which results in a generally non-smooth contact pressure distribution.

In paper [8] the optimum shape of a roller bearing is determined by the control function according to formulae (3.3)-(3.5), in which $f_2 = f_3 = 1$. The roller has a

translation and rigid body rotation. In the optimization process the rolling state of the roller has not been taken into account, that is, there is no friction.

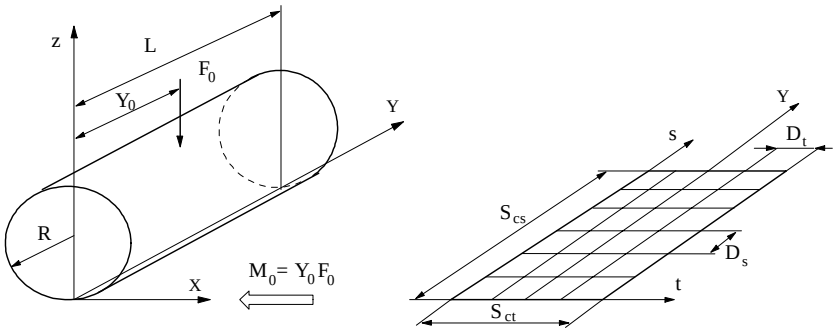

Figure 10. Roller load and geometrical properties

A roller is loaded by the force F_0, which can be replaced by an equivalent force couple system F_0 and M_0 on the axis x. The geometry and the load of a roller can be found in Figure 10. The elastic half-space model is applied to produce the influence function for the roller, taking the mirror technique [9] into account. $Z = 0$ on the surface of the half-space and the rectangular contact region $(S_{ct} \times S_{cs})$ is divided into small rectangles $(D_t \times D_s)$.

Elements of the influence matrix are computed by applying a unit normal load or a unit tangential load in the direction X in the sub-region $D_t \times D_s$. The formulae can be found in Kalker's book [19]. In order to eliminate shearing stresses at the ends of the roller, the mirror technique is taken into account.

The present work enhances the previous results in two ways.

1. Firstly, if the load is not applied along the center of the roller, that is $Y_0 < \frac{S_{cs}}{2}$, an algorithm should be applied, which is based on the following formula
$$M_* = Y_0 \int\limits_{\Omega} p\, dS - \int\limits_{\Omega} Y p\, dS\,, \tag{3.27}$$
which should be minimized to zero.
   In this case there are two possibilities.
   - The first is to search for the end of the control function, that is $s = L_4$, when $f_2 = f_3 = 1$ and the value of B is practically zero. The result is that the contact pressure is carried by the $0 \le s \le L_4$ interval of the roller.
   - The second is to ensure contact along the roller's full length. In this case the problem is to search for the value $f_3 < 1$, while $f_2 = 1$.
2. Secondly, the tangential components of stress are taken into account while optimizing the shape of the roller, when the roller is loaded in its center. The pressure distribution is controlled by parameters L_j, $j = 1, \ldots, 4$ during optimization, using the control functions defined under (3.4).

To solve the rolling problem Kalker's program [30] is used, which is written in FORTRAN. The calculations use the KOMBI subroutine of Kalker's program, which gives a prescribed F_0 load, and a prescribed displacement in direction X. The theoretical background of the program can be found in work [19].

3.3.1. *Examples for non-centrally loaded rollers.* The radius of the roller is $R_0 = 60\,mm$. The roller is subjected to loads of $F_0 = 5000\,N$ and $M_0 = 33000\,Nmm$; $Y_0 = 13.2\,mm$. The material properties are as follows: Young modulus: $E = 1.97{\cdot}10^5\,MPa$, Poisson ratio: $\mu = 0.28$.

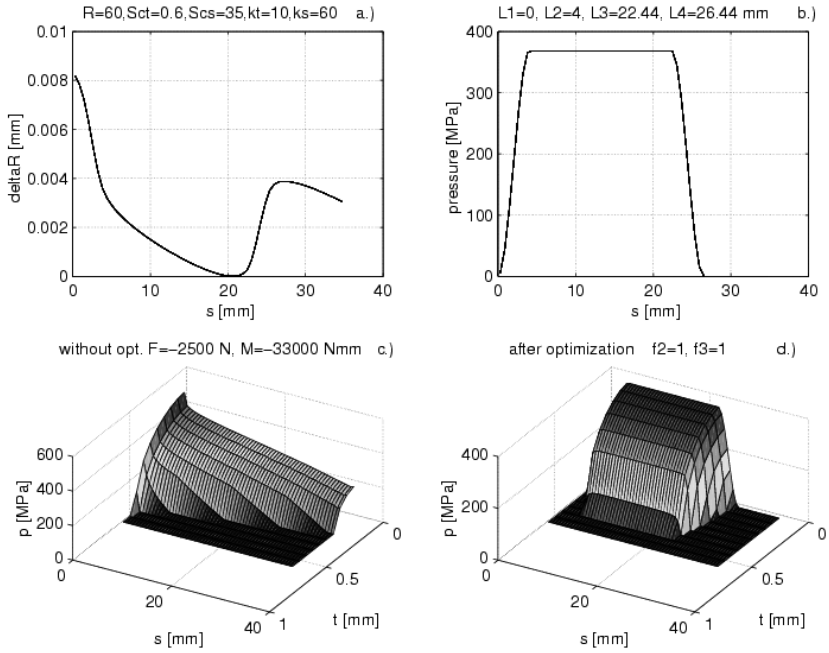

Figure 11. Optimized shape and pressure distribution in the 2^{nd} solution

The proposed contact region is divided into $10 \cdot 60$ rectangular elements, $L_1 = 0\,mm$, $L_2 = 4\,mm$, $L_4 - L_3 = 4\,mm$. In this case $n = 12$ (see formula (3.5))

- *First solution:* The problem can be solved by making use of an algorithm published in [8]. At the end of the calculations $M_* = -77.7\,Nm$, $B = -0.999$, $L_4 = 26.86\,mm$ and $p_{\max} = 369.1\,MPa$.
- *Second solution:* For the first case the value of $L_4$is determined by positive pressure. However, for the the second case L_4 is determined by the minimization of the moment M_*. The algorithm developed gave the following results: $M_* = -6.65\,Nm$, $B = -0.68 \cdot 10^{-3}$, $L_4 = 26.44\,mm$ and $p_{\max} = 368.9\,MPa$.

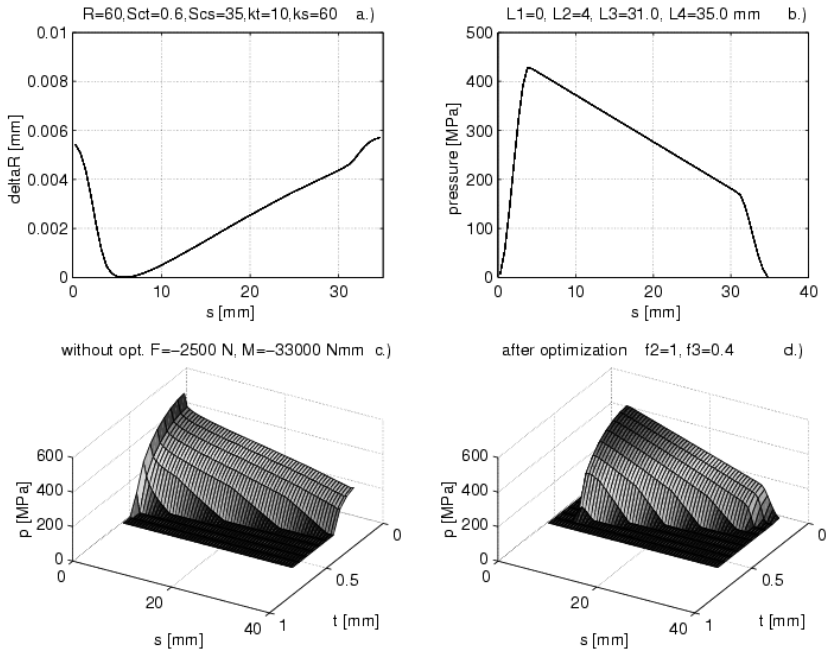

Figure 12. Optimized shape and pressure distribution in the 3^{rd} solution

Figure 11 shows the initial gap, the pressure distribution in the central longitudinal section of the roller, and the pressure over the whole domain before and after optimization.

- *Third solution:* The value of moment M_* is minimized by changing the parameter f_3, while equation $L_4 = S_{cs}$ is kept. Results of the calculation are $M_* = 47.58\,Nm$, $B = 0.39 \cdot 10^{-3}$ and $p_{\max} = 425\,MPa$. Figure 12 shows the initial gap and the stress-state for this optimization prioblem.

  Comparing these results, it can be realized that the second solution is the best according to the objective function ($\min p_{\max}$).

3.3.2. *Optimization of centrally loaded rollers when rolling.* The equilibrium equations for the roller are of the form

$$\mathbf{F} = \mathbf{F}_0 - \int_\Omega \mathbf{p}\, dS = \mathbf{0}\,, \qquad \mathbf{M} = \mathbf{M}_0 - \int_\Omega \mathbf{R} \times \mathbf{p}\, dS = \mathbf{0}\,, \tag{3.28}$$

where $\mathbf{p}$ is the contact stress acting on the second body, $\mathbf{R}$ is the position vector, $\mathbf{F}_0$, $\mathbf{M}_0$ are the resultant and moment resultant of the load exerted on the roller. The

optimization problem can be written as follows

$$\min\Big\{p_{\max}\,\Big|\,p\geq 0,\ d\geq 0,\ p\cdot d=0,\ \textsf{Coulomb frict. cond.},\ \mathbf{x}\in\Omega\,,\\ \chi=0,\ \mathbf{x}\in\Omega_c,\ \chi\geq 0,\ \mathbf{x}\in\Omega_{nc},\ \mathbf{F}=\mathbf{0},\ \mathbf{M}=\mathbf{0}\Big\},\tag{3.29}$$

where friction conditions are taken into consideration in the rolling motion.

Minimization is solved by using an iteration process. The effect of tangential stress, which is calculated in the rolling problem, is taken into account when determining the displacement in the normal direction during the minimization of the maximum pressure. Therefore the normal displacement from tangential stress p_τ along the direction X is

$$\widetilde{u}_N^\alpha(\mathbf{x})=(-1)^\alpha\int\limits_\Omega H^{(\alpha)\,NT}(\mathbf{x},\mathbf{s})\,p_\tau(\mathbf{s})\,dS\,,\qquad \alpha=1,2,\tag{3.30}$$

where $H^{(\alpha)\,NT}(\mathbf{x},\mathbf{s})$ is the Green-influence function in the α^{th} body.

The normal displacement due to the pressure is as follows

$$u_N^\alpha(\mathbf{x})=(-1)^\alpha\int\limits_\Omega H^{(\alpha)\,NN}(\mathbf{x},\mathbf{s})\,p(\mathbf{s})\,dS\,.\tag{3.31}$$

The displacement difference along normal direction can be written as

$$u_N^2-u_N^1=\int\limits_{S_c}\Big(H^{(1)\,NN}(\mathbf{x},\mathbf{s})+H^{(2)\,NN}(\mathbf{x},\mathbf{s})\Big)p(\mathbf{s})\,dS+\widetilde{u}_N^{(2)}-\widetilde{u}_N^{(1)}-u^1_{\textsf{rigid}}=\tag{3.32}$$

$$=\sum_{\alpha=1}^{2}\int\limits_{S_c}H^{(\alpha)\,NN}(\mathbf{x},\mathbf{s})\,p(\mathbf{s})\,dS+\sum_{\alpha=1}^{2}\int\limits_{S_c}H^{(\alpha)\,NT}(\mathbf{x},\mathbf{s})\,p_\tau(\mathbf{s})\,dS-u^1_{\textsf{rigid}}\,.$$

where $u^1_{\textsf{rigid}}$ is the normal displacement from the rigid body motion of the roller (translation along z and rotation around X).

The radius of the roller is

$$R=R(t),\tag{3.33}$$

which is used to determine the initial gap $h(\mathbf{x})=h(x,t)=h(x,R(t))$ between the bodies. The optimization problem is solved by the iterational method. The following sub-optimization problem is defined, in which the optimized shape is calculated with the control of the contact pressure, where the effect of the tangential stress p_τ on the normal displacement is taken into account. The rolling problem is calculated with the use of the optimized shape, then p_τ is determined and is used to solve the sub-optimization problem again. The optimization problem for calculating the change in radius can be written in the following way

$$\min\Big\{p_{\max}\,\Big|\,p\geq 0,\ d=d(p,p_\tau\ \textsf{is fixed},R)\geq 0,\ p\cdot d=0\,,\\ \chi(p)\geq 0,\ \mathbf{F}=\mathbf{0},\ \mathbf{M}=\mathbf{0}\Big\}.\tag{3.34}$$

In this task p, $p_{\max}$ and R are unknown variables. The discretized problem is solved by using the iteration recommended in [9].

In the pressure control the change in radius will only be significant in the subdomain Ω_E, which is associated with the end of the roller. In this domain the resultant tangential stress is

$$T = \int\limits_{\Omega_E} p_\tau \, dS \,. \tag{3.35}$$

The iteration continues until the following error limit holds true

$$\frac{|T^{(\mathsf{irol})} - T^{(\mathsf{irol}-1)}|}{|T^{(\mathsf{irol})}|} 100 \leq 0.05 \,. \tag{3.36}$$

The iterational algorithm has the following structure

```
LOOP over rolling:  irol=1,...,k convergence
    if (irol .eq.  1) call pressure optimization loop
    Solving the Rolling contact problem with Kalker's program.
    LOOP over pressure optimization:  igap=1,..., convergence
                Solving the optimization problem (3.34)
    END LOOP
    Convergence:  when tolerance (3.36) holds true
 END LOOP
```

3.3.3. *Numerical example.* The roller and an elastic half-space are observed. The radius of the roller is $R = 60\,mm$. The roller is subjected to loads of $F_0 = 5\,kN$ and $M_0 = 87.5\,kNmm$. The proposed zone of the contact region is given by $S_{ct} = 1mm \times S_{cs} = 35mm$, and it is divided into 18×30 rectangular elements, $f_2 = f_3 = 1$, $L_1 = 0\,mm$, $L_2 = 4\,mm$, $L_4 - L_3 = 4\,mm$. The static and kinetic coefficient of friction is $\mu_0 = 0.2$in this example. The displacement of the roller's centerline along the direction X is prescribed as $u_x = 0.005mm$.

Figure 13 the pressure distribution can be seen with and without optimization. The optimized gap is illustrated in section *a.)* of the Figure.

Figure 14 shows the contact stress, pressure (p), tangential stress (Tau $\equiv p_\tau$) in the direction X and the slip function in the contact region. The slip function ($\hat{s}$), illustrated in Figure 14, is calculated by Kalker's routines, which provide the function with reference to the velocity of the roller's center point, and $\hat{s}$ has a value with no dimension. The radius of the roller is R_0, and the velocity of the roller's center point is V_0, i.e. $\omega = \frac{V_0}{R_0}$.

4. **Optimization of roller shape and wear**

The rolling element and the base are in contact and there is a slip area between them, since the surface of the contacting elements undergoes wear. The speed of wear

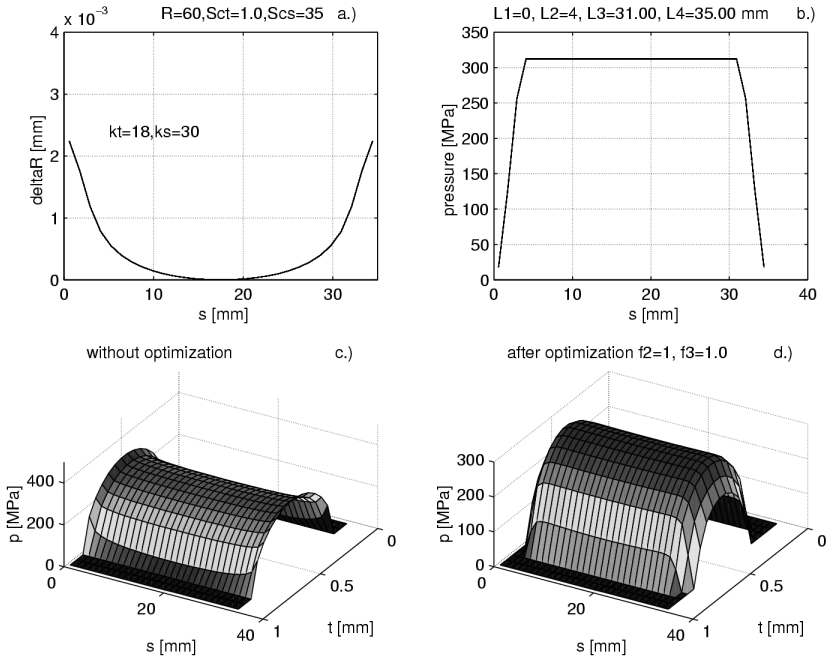

Figure 13. Optimized gap, control function and pressure with and without optimization

is defined by

$$\dot{w} = C\mu\, p\, ||\dot{\mathbf{u}}_\tau|| = C\mu\, p\, \hat{s}\, V_0 = C\mu\, p\, \hat{s}\, R_0\, \omega\,, \tag{4.1}$$

where C is a material property and $\hat{s}$ is the slip, when the rolling velocity is equal to one.

Since the roller rotates while moving forward, the total wear is calculated by the time integration of equation (4.1) by taking the rotational time ($t_\omega = \frac{2\pi}{\omega}$) into account. During time t_* the total wear which exerts an influence on changing the radius is

$$W = \int_0^{\frac{t_*}{t_\omega}} \int_\Omega C\mu\, p\hat{s} R_0 \omega\, d\Omega\, d\tau = \int_0^{\frac{t_*}{t_\omega}} \int_\Omega \widetilde{C}\mu\, p\hat{s}\, d\Omega\, d\tau\,, \tag{4.2}$$

where $\widetilde{C} = CR_0\,\omega$. During the rolling motion the roller is moving along direction X. It is supposed that the wear is evaluated for a Y co-ordinate of the roller by the integral of the $\mu\, p$ and $\hat{s}$ quantities which can change along the direction X, that is

$$W = \int_0^{\frac{t_*}{t_\omega}} \int_0^{S_{cs}} \int_0^{S_{ct}} C\mu\, p(s,t)\hat{s}(s,t)\, dt\, ds\, d\tau\,. \tag{4.3}$$

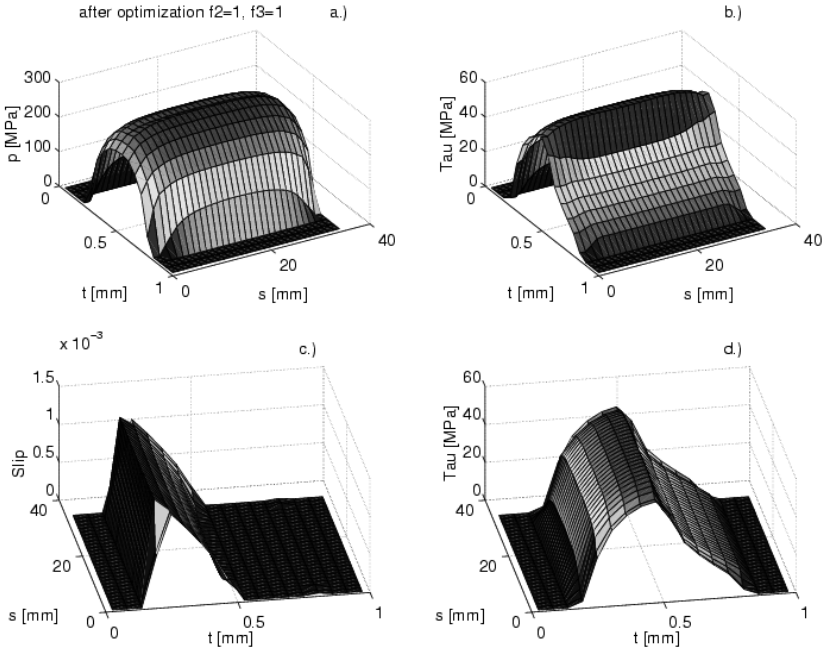

Figure 14. Optimized pressure $\mathbf{p}$, $\mathbf{p}_\tau$ and slip distribution in rolling state

The contact region is divided into small rectangles with size $D_s \times D_t$. There are KX, along the direction X, and KY, along the direction Y, pieces of rectangles. All of the rectangles may have various contact stresses and relative speeds, which are calculated in the middle of these small areas. These quantities are supposed to be constant within the rectangles. In this way the formula (4.3) can be rewritten as

$$W = \int_0^{\frac{t_*}{t_\omega}} \Big(\sum_{j=1}^{\mathsf{KY}} \sum_{i=1}^{\mathsf{KX}} C\mu\, p_{ij} \hat{s}_{ij} D_s D_t \Big)\, d\tau, \tag{4.4}$$

where $p_{ij} = p(s_i, t_j)$, and $\hat{s}_{ij} = \hat{s}(s_i, t_j)$.

During the time integration it is supposed that the pressure and slip vary linearly between τ_n and τ_{n+1} time, which define an interval ${}^{n+1}_{n}\Delta = \tau_{n+1} - \tau_n$. Introducing the parameter $0 \le \Theta \le 1$ the pressure is formulated as

$$p_{ij} = (1 - \Theta) p_{ij}^n + \Theta\, p_{ij}^{n+1}, \tag{4.5}$$

where p_{ij}^n, p_{ij}^{n+1} are pressure at time τ_n, τ_{n+1}. Similar equation can be written for slip too. With the use of (4.5) the following formula can be written

$$\begin{aligned}\int_{\tau_n}^{\tau_{n+1}} p_{ij}\hat{s}_{ij}\,d\tau &= {}^{n+1}_{n}\Delta\Big[\frac{1}{3}\big(p_{ij}^n\,\hat{s}_{ij}^n + p_{ij}^{n+1}\,\hat{s}_{ij}^{n+1}\big) + \frac{1}{6}\big(p_{ij}^n\,\hat{s}_{ij}^{n+1} + p_{ij}^{n+1}\,\hat{s}_{ij}^n\big)\Big] \\ &\equiv {}^{n+1}_{n}\Delta\;{}^{n+1}_{n}B_{ij}\end{aligned} \tag{4.6}$$

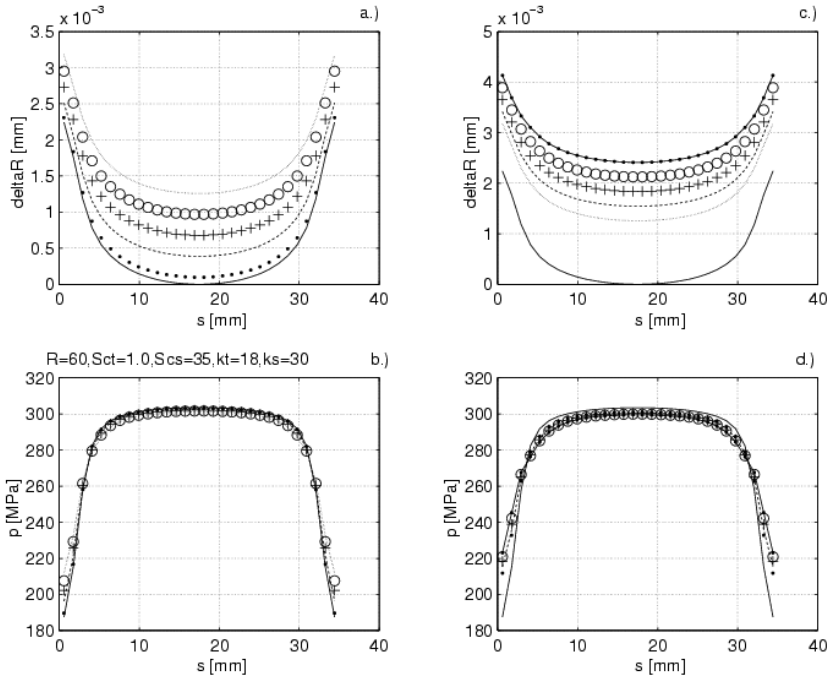

Figure 15. Change in the radius roller

The change in the radius of the roller is

$${}^{n+1}_{n}(\Delta R_j) = \sum_{i=1}^{\mathsf{KX}} {}^{n+1}_{n}B_{ij}\hat{C}D_sD_t\,, \qquad j = 1,\ldots,\mathsf{KY}, \tag{4.7}$$

where $\hat{C} = {}^{n+1}_{n}\Delta\,\widetilde{C}$, and it is calculated in section s_j and ${}^{n+1}_{n}\Delta$ time-interval.

After wear the new radius of the roller can be written as follows

$${}^{n+1}R_j = {}^{n}R_j - {}^{n+1}_{n}(\Delta R_j), \qquad j = 1,\ldots,\mathsf{KY}. \tag{4.8}$$

Figure 15 illustrates the results of a numerical calculation for the wearing process. In sub-figures the symbols stand for the times steps. In *a.*) and *b.*) chars have the following meanings; $-$: optimal shape, $..$: 1^{st} time step, $--$: 2^{nd} time step, $++$:

3^{rd} time step, $\circ\circ$: 4^{th} time step, ...: 5^{th} time step. In of diagrams *c.*) and *d.*) symbols have the meaning: $-$: optimal shape, ...: 5^{th} time step, $--$: 6^{th} time step, $++$: 7^{th} time step, $\circ\circ$: 8^{th} time step, $\bullet$–: 9^{th} time step, the value of parameter $\hat{C}$ is 0.025.

5. Conclusion

Contact optimizations using the control of contact pressure have been performed for many problems. Three groups of contact optimization tasks have been examined.

- In the first group axially symmetric contact problems have been solved by p-extension finite elements. Discretization of the domain with these elements is advantageous, since it results in fast convergence, and high order mapping assures accurate geometry for shape optimization.

  The following contact optimization problems have been solved for axisymmetric bodies:

  1. Minimizing the maximum of contact pressure (Problems P1, P3)
  2. Maximizing the rigid body displacement (Problem P2)
  3. Maximizing the contact resultant force (Problem P4)
  4. Maximizing the torque due to friction (Problems P5, P6)
  5. Minimizing the frictional power loss (Problems P7, P8)
  6. Minimizing the wearing velocities (Problem P9)

- In the second group of optimization problems an optimal shape design of the roller has been carried out. A new control function and three algorithms are proposed.

- In the third group of optimization problems the roller is loaded centrally and the rolling state has been taken into account. A special iterational algorithm has been developed for solving the rolling contact optimization problem. The rolling problem has been solved with Kalker's subroutines in order to calculate the shearing stresses. The influence of friction is not significant and the examples demonstrate the effectiveness of the proposed algorithms.

  Finally, a numerical method is developed for solving the problem of wear. The wearing process is analyzed for a moving roller with optimized shape.

Acknowledgement. We thank professor J. Kalker for the opportunity to utilize the source code calculating the rolling problem. Financial support for this paper was provided by Grants FKFP 0040/1999 and OTKA T025172.

REFERENCES

1. Mróz, Z.: *Sensitivity analysis of distributed and discretized systems*, Advanced TEMPUS Course on Numerical Methods in Computer Aided Optimal Design, Zakopane, May 11-15, 1992, T. Burczynki [Ed.] Silesian Technical University of Gliwice, Lecture Notes, **Vol. 1.** 1-60, (1992)

2. Klarbring, A.: *Contact, Friction, Discrete Mechanical Structures and Mathematical Programming.* In CISM course: Contact problems: Theory, Methods, Applications, pp. 1-51, Udine, 1997.
3. Hilding, D., Klarbring, A. and Petersson J.: *Optimization of structures in unilateral contact*, Appl. Mech. Rev. **52**(4), (1999), 139-160.
4. Haslinger, J. and Neattaanmaki, P.: *Finite Element Approximation for Optimal Shape Design*, John Wiley & Sons Ltd., London, 1996.
5. Páczelt, I. and Szabó, T.: *Application of the augmented lagrangian technique for solution of contact optimization problems.* In M. Aliabadi and C. Alessandri, editors, Second International Conference Contact Mechanics: Contact Mechanics II, pp. 249-256, Computational Mechanics Publications, London, 1995.
6. Páczelt, I.: *Some new developments in contact pressure optimization*, Engng. Trans., **43**(1-2), (1995), 297-312.
7. Páczelt, I. and Szabó, T.: *Solution of contact optimization problems of cylindrical bodies using the hp-FEM*, Int. J. Numer. Meth. Engng., **53**, (2002), 123-146.
8. Páczelt, I.: *Iterative methods for solution of contact optimization problems*, Arch. Mech., **52**(4-5), (2000), 685-711.
9. Páczelt, I. and Szabó, T.: *Optimal shape design for contact problems*, Structural Optimization, **7**(1/2), (1994), 66-75.
10. Benedict, R. L. and Taylor, J. E.: *Optimal design for elastic bodies in contact*, In Optimization of distributed parameters structures, Part II., E. J. Haug, J. Cea, 1553-1599, Sijthoff and Alphen an den Rijn, 1981.
11. Kikuchi, N. and Taylor, J.E.: *Shape optimization for unilateral elastic contact problems*, In Num. Meth. Coupl. Probl. (Proc. Int. Conf., held at University College, Swansea, Wales), 430-441, 1981.
12. Klarbring, A.: *On the problem of optimizing contact force distributions*, J. Optimization Theory Appl., **74**, (1992), 131-150.
13. Klarbring A. and Haslinger J.: *On almost constant stress distributions by shape optimization*, Structural Optimization, **5**, (1993), 213-216.
14. Conry, I. F. and Seireg, A.: *A mathematical programming method for design of elastic bodies in contact*, J. Appl. Mech. **38**, (1991), 387-392.
15. Oda J., Sakamoto J. and San, K.: *A method for producing a uniform stress distribution in composite with interface*, Structural Optimization, **3**, (1991), 23-28.
16. Páczelt, I. and Herpai, B.: *Some remarks on the solution of contact problems of elastic shells*, Archivum Budowy Maszyn XXIV, (1977), 197-202.
17. Peterson, J.: *Behaviorally constrained contact force optimization*, Structural Optimization, **9**, (1995), 189-193.
18. Szabó, B. and Babuska I.: *Finite Element Analysis*, Wiley-Interscience, New-York, 1991.
19. Kalker J.J.: *Three Dimensional Elastic Bodies in Rolling Contact*, Academic Publisher, Doordrecht, 1990.
20. Béda Gy., Kozák I. and Verhás J.: *Continuum Mechanics*, Academic Publisher, Budapest, 1995.

21. Fancello, E.A. and Feijóo, R.A.: *Shape optimization in frictionless contact problems*, Int. J. Numer. Meth. Engng., **37**, (1994), 2311-2335.

22. Fancello E., Haslinger, J. and Feijóo, R. A.: *Numerical comparison between two cost functionals in contact shape optimization*, Structural Optimization, **9**, (1995), 57-68.

23. Herskovits J., Leontiev A., Dias G. and Santos G.: *Contact Shape Optimization: A bilevel programming approach*, Struc. Multidisc. Optim., **20**, (2000), 214-221.

24. Páczelt, I., Szabó, B. and Szabó, T.: *Solution of contact problem using the hp-version of the finite element method*, Computers and Mathematics with Application, **38**, (1999), 49-69.

25. Strömberg, N., Johanson, L. and Klarbring, A.: *Derivation and analysis of a generalized standard model for contact, friction and wear*, Int. J. Solids Structures, **33**, (1996), 1817-1836.

26. Oh, K. P. and Trachmann, E. G.: *A numerical procedure for designing profiled rolling*, ASME J. Lubrication Technology Series F, **98**, (1996), 68-75.

27. Harnett, M. J.: *The analysis of contact stresses in rolling element bearings*, Trans. ASME, J. Lubrication Technology Series F, **101**, (1979), 105-109.

28. Chiu, Y. P. and Harnett, M. J.: *A numerical solution for the contact problem involving bodies with cylindrical surface considering cylinder effect*, ASME J. Tribology, **109**, (1987), 479-486.

29. de Mul, J. M., Kalker, J.J. and Frederiksson B.: *The contact between arbitrarily curved bodies of finite dimension*, ASME J. Tribology, **108**, (1986), 140-148.

30. Kalker, J.J.: CONPC90*, User's Manual, Listing CONPC*, TU Delft, Faculty of Technical Mathematics and Informatics, 1982, 1986, 1990.